

# Numerical simulation of the flow topology over NREL's S807 airfoil at different models of turbulence

Pavlo Kosiak<sup>1,2,\*</sup>, Vitalii Yanovych<sup>1,2</sup>, Václav Uruba<sup>1,2</sup> and Daniel Duda<sup>1</sup>

<sup>1</sup>Power System Engineering, Faculty of Mechanical Engineering, University of West Bohemia in Pilsen, Univerzitní 22, 306 14 Pilsen, Czech Republic.

<sup>2</sup>Department of Fluid Dynamics, Institute of Thermomechanics, Czech Academy of Sciences, Dolejškova 5, 182 00, Prague, Czech Republic

**Abstract.** Current numerical simulations investigate subsonic flow around the NREL's S807 airfoil without an incident angle at Reynolds numbers near  $2.8 \cdot 10^5$ . This work is devoted to the assessment application of various turbulence models for a numerical simulation of the formed flow around the streamlined body in commercial software ANSYS CFX. Namely, we applied Shear Stress Transport fully turbulent model (SST0, Baseline Reynolds stress model (BSL RSM) and SSG RSM for the computation of velocity deficit, degree of turbulence anisotropy, Reynolds stress components, and aerodynamic performance of the airfoil. The obtained results were validated on the basis of hot wire measurement data. Additionally, in order to validate the obtained results, a comparison with the hot-wire experimental data was also carried out. The obtained experimental and calculated data showed some differences in the wake topology. For example, in the case of hot-wire data, there is a smaller velocity deficit and a wider area of perturbation.

## 1 Introduction

The structure of the flow behind and around the wind airfoils plays a big role during the operation of the wind turbine blades, which includes these airfoils. Nowadays the development of computer technology makes it possible to conduct qualitative research using CFD (Computational Fluid Dynamics) simulation. A lot of papers were published where the authors show examples of using CFD.

For example, Eleni Douvi, Dionissios P. Margaritis, and T. I. Athanasios in the paper [1] performed the simulation of the flow around the symmetrical airfoil NACA 0012 using different models of turbulence:  $k-\omega$  SST,  $k-\varepsilon$  Realizable, and others. This article [1] shows the dependences of drag and lift coefficients on the angle of attack for different models of turbulence. The paper [1] shows that model of turbulence  $k-\omega$  SST good agreement with experimental data. Also, the results of the investigation of the flow around the airfoil NACA 0012 are described in the literature [2]. The authors of this paper performed the simulation for different sizes of the fluid domain in the  $z$ -direction. It was shown that the best results were obtained using a fluid domain with a size in the  $z$  direction equal to the airfoil chord [2].

Also, the CFD simulation of different symmetrical and non-symmetrical airfoils was shown in the literature [3]. The authors performed the simulation using the commercial software ANSYS Fluent. This paper shows that with increasing the Reynolds number, the lift coefficient increases, and the drag coefficient decreases. Also, the article [3] represents the influence of the camber value on the lift and drag coefficient.

The aim of this paper show functionality of two models of turbulence: Shear Stress Transport fully turbulent and the Baseline Stress model. The investigation was performed using ANSYS CFX commercial software. The flow was searched behind the asymmetrical airfoil NREL's S807 with chord  $c \approx 100$  mm for  $U=40$  m·s<sup>-1</sup> inlet velocity and zero degree angle of attack using three models of turbulence: the Baseline Reynolds stress model (BSL RSM), SSG RSM and the Shear Stress Transport fully turbulent model (SST). The flow was searched behind the airfoil at cross-section, which is 100 mm from trailing edge.

## 2 CFD simulation

CFD simulations were performed using ANSYS CFX commercial software. Despite the low inlet velocity 40 m·s<sup>-1</sup>, the flow was modeled as compressible using the ideal gas material model and total energy model.

Numerical simulations were performed using three models of turbulence: the Baseline Reynolds stress model (BSL RSM) and the Shear Stress Transport fully turbulent model (SST).

The SST (Shear Stress Transport) model of turbulence was created as a combination of the two models:  $k-\varepsilon$  and  $k-\omega$ . Using special function  $F_1$  described model can activate the  $k-\omega$  model near the wall and  $k-\varepsilon$  at the free stream. For activating the  $k-\omega$  model  $F_1=1$  and for  $k-\varepsilon$   $F_1=0$  [4]. The SST model, also, accounts the transport of the turbulent shear stress  $\tau = -\rho \overline{u'v'}$  using equation (1) [5].

$$\frac{D\tau}{Dt} = \frac{\partial \tau}{\partial t} + u_k \frac{\partial \tau}{\partial x_k} \quad (1)$$

where  $\rho$  is density of the fluid,  $u', v'$  are velocity fluctuations of  $u$  and  $v$  components of velocity.

The SST model of turbulence includes two transport equations: for turbulent kinetic energy  $k$  (2) and for parameter  $\omega$  (3), which characterizes the dissipation of  $k$  [6].

$$\frac{\partial(\rho k)}{\partial t} + \frac{\partial(\rho \bar{U}_j k)}{\partial x_j} = P_k - D_k + \frac{\partial}{\partial x_j} \left[ (\mu + \sigma_k \mu_t) \frac{\partial k}{\partial x_j} \right] \quad (2)$$

$$\begin{aligned} \frac{\partial(\rho \omega)}{\partial t} + \frac{\partial(\rho \bar{U}_j \omega)}{\partial x_j} = & P_k \frac{\alpha}{\nu_t} - \beta \rho \omega^2 + \frac{\partial}{\partial x_j} \left[ (\mu + \sigma_\omega \mu_t) \frac{\partial \omega}{\partial x_j} \right] \\ & + (1 - F_1) 2 \rho \sigma_\omega \frac{1}{\omega} \frac{\partial k}{\partial x_j} \frac{\partial \omega}{\partial x_j} \end{aligned} \quad (3)$$

where  $P_k$  and  $D_k$  are production and destruction terms of the turbulent kinetic energy respectively.

The SSG RSM models is one of three standard Reynolds Stress models, which are based on the  $\varepsilon$ -equation (6) [7].

$$\begin{aligned} \frac{\partial(\rho \varepsilon)}{\partial t} + \frac{\partial(\rho U_k \varepsilon)}{\partial x_k} = & \frac{\varepsilon}{k} (C_{\varepsilon 1} P_k - C_{\varepsilon 2} \rho \varepsilon + C_{\varepsilon 1} P_{\varepsilon b}) \\ & + \frac{\partial}{\partial x_k} \left[ \left( \mu + \frac{\mu_t}{\sigma_{\varepsilon RS}} \right) \frac{\partial \varepsilon}{\partial x_k} \right] \end{aligned} \quad (4)$$

This equation (4) includes the anisotropy diffusion coefficient from the original model, but this term have been replaced by an isotropy term [7].

Also, the Reynolds Stress model solves the transport equation for (5) for Reynolds stresses [7]:

$$\begin{aligned} \frac{\partial(\rho \overline{u_i u_j})}{\partial t} + \frac{\partial}{\partial x_k} (U_k \rho \overline{u_i u_j}) - \frac{\partial}{\partial x_k} \left[ \left( \delta_{kl} \mu + \rho C_s \frac{k}{\varepsilon} \overline{u_k u_l} \right) \frac{\partial \overline{u_i u_j}}{\partial x_k} \right] \\ = P_{ij} - \frac{2}{3} \rho \varepsilon \delta_{ij} + \Phi_{ij} + P_{ij,b} \end{aligned} \quad (5)$$

where  $\Phi_{ij}$  is the pressure-strain correlation, and  $P_{ij}$  is exact production term [7]. Speziale, Sarkar and Gatski developed the SSG RSM model and they used a quadratic relation for the pressure-strain correlation [7]. Pressure strain correlations in general form are (6), (7) [7]:

$$\Phi_{ij,1} = -\rho \varepsilon \left[ C_{s1} a_{ij} + C_{s2} \left( a_{ik} a_{kj} - \frac{1}{3} a_{mn} a_{mn} \delta_{ij} \right) \right] \quad (6)$$

$$\begin{aligned} \Phi_{ij,2} = & -C_{r1} P a_{ij} + C_{r2} \rho k S_{ij} - C_{r3} \rho k S_{ij} \sqrt{a_{mn} a_{mn}} \\ & + C_{r4} \rho k \left( a_{ik} S_{jk} + a_{jk} S_{ik} - \frac{2}{3} a_{kl} S_{kl} \delta_{ij} \right) \\ & + C_{r5} \rho k (a_{ik} \Omega_{jk} + a_{jk} \Omega_{ik}) \end{aligned} \quad (7)$$

where:

$$a_{ij} = \frac{\overline{u_i u_j}}{k} - \frac{2}{3} \delta_{ij} \quad (8)$$

$$S_{ij} = \frac{1}{2} \left( \frac{\partial u_i}{\partial x_j} + \frac{\partial u_j}{\partial x_i} \right) \quad (9)$$

$$\Omega_{ij} = \frac{1}{2} \left( \frac{\partial u_i}{\partial x_j} - \frac{\partial u_j}{\partial x_i} \right) \quad (10)$$

where:  $C_{s1} = 1.7$ ,  $C_{s2} = -1.05$ ,  $C_{r1} = 0.9$ ,  $C_{r2} = 0.8$ ,  $C_{r3} = 0.65$ ,  $C_{r4} = 0.625$  and  $C_{r5} = 0.2$

Baseline Reynolds Stress model (BSL RSM) based solving the transport equation of Reynolds stresses (11) and transport equation for  $\omega$  (12) [7].

$$\frac{\partial(\rho \overline{u_i u_j})}{\partial t} + \frac{\partial}{\partial x_j} (U_k \rho \overline{u_i u_j}) = P_{ij} - \frac{2}{3} \rho \omega k \delta_{ij} + \Phi_{ij} +$$

$$P_{ij,b} + \frac{\partial}{\partial x_k} \left[ \left( \mu + \frac{\mu_t}{\sigma_k} \right) \frac{\partial \overline{u_i u_j}}{\partial x_k} \right] \quad (11)$$

$$\begin{aligned} \frac{\partial(\rho \omega)}{\partial t} + \partial(\rho U_k \omega) = & \{ \alpha_3 \frac{\omega}{k} P_k + P_{\omega b} - \beta_3 \rho \omega^2 \\ & + \frac{\partial}{\partial x_k} \left[ \left( \mu + \frac{\mu_t}{\sigma_{\omega 3}} \right) \frac{\partial \omega}{\partial x_k} \right] \\ & + (1 - F_1) 2 \rho \frac{1}{\sigma_{2\omega}} \frac{\partial k}{\partial x_k} \frac{\partial \omega}{\partial x_k} \end{aligned} \quad (12)$$

Thanks to BSL RSM and SSG RSM model is possible to determine variation of velocity fluctuations.

3D Flow domain with  $745 \times 305 \times 1$  mm (see Figure 1) sizes was created using SpaceClaim software, which is part of ANSYS.

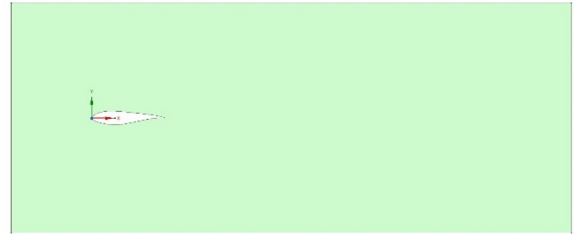


**Fig. 1.** Fluid domain around the airfoil.

The simulating mesh was creating using ICEM CFD, which is, also, part of ANSYS. Fig.2 shows the detail of the mech around the airfoil.

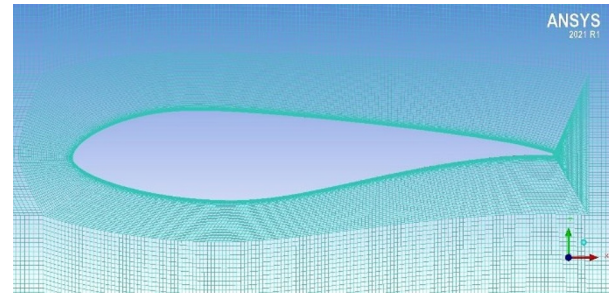


**Fig. 2.** Fluid domain around the airfoil.

Simulated mesh contains 1007385 cells. The value of  $y^+$  around the airfoil is much less than 1, that's why the high of the first layer of cells around the profile is between  $4 \times 10^{-7} - 8 \times 10^{-7}$  m.

Simulation was performing like steady-state using ANSYS CFX comercial. The flow was modeled like compresible, that's why total energy option was used and air was simulated like ideal gas. As for boundary conditions: velocity-inlet and static pressure-outlet were used. Simulations were performed for inlet velocity  $U = 40$  m/s ( $Re \approx 2.8 \times 10^5$ ) and 0 degree of inlet angle. Also, inlet boundary condition contains intensity of turbulence, 0.2 %, eddy viscosity ratio 15 and static temperature 24 °C. Outlet boundary condition includes static pressure 98500 Pa.

### 3 Results

Figure 3, Figure 4 and Figure 5 show simulated flow field using SST fully turbulent and BSL RSM and SSG RSM models of turbulence with  $U=40$  m/s inlet velocity

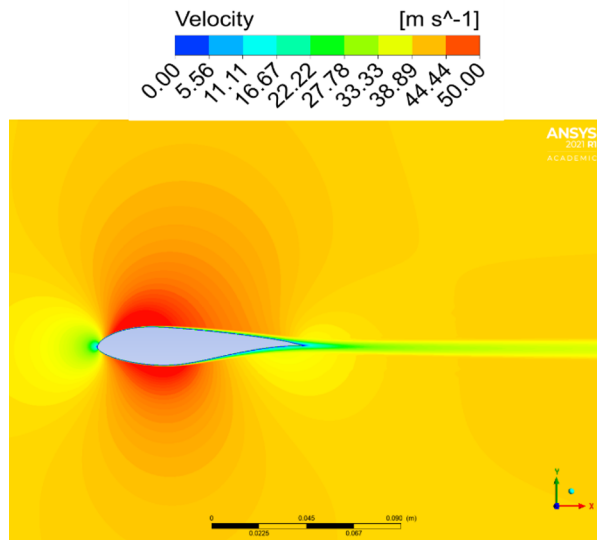


**Fig. 3.** Simulated flow field with using SST fully turbulent model of turbulence.

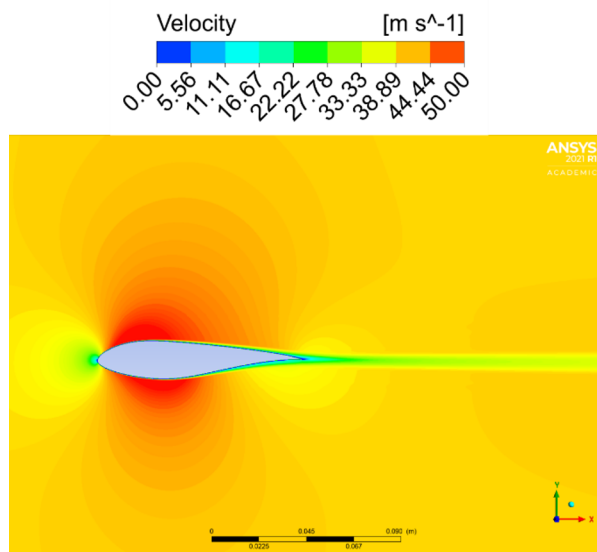


**Fig. 4.** Simulated flow field with using BSL RSM model of turbulence.

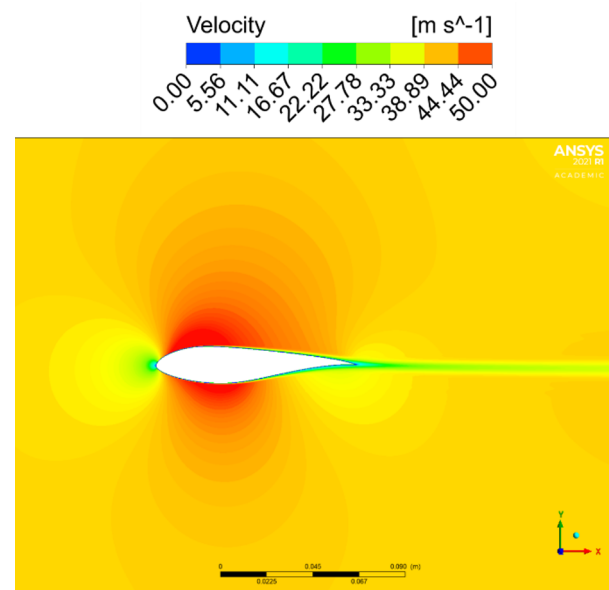


**Fig. 5.** Simulated flow field with using SSG RSM model of turbulence.

The flow fields received by using three different models of turbulence are similar.

All profiles then were obtained in cross-section behind the airfoil at 100 mm from trailing edge and in range of  $y \cdot c^{-1}$  from -0.5 to 0.5, where  $y$  is coordinate of search points,  $c$  is chord of airfoil.

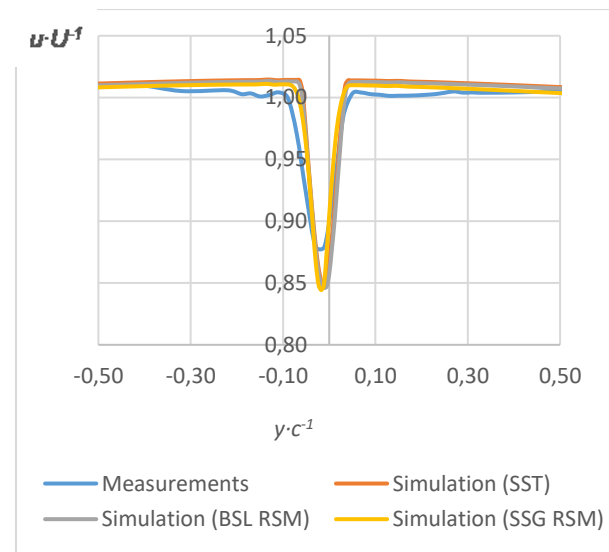


**Fig. 6.** Normalized profiles of stream-wise component of the mean velocity.

Figure 6 shows normalized profiles of stream-wise component of mean velocity obtained by simulation with using SST, BSL RSM and SSG RSM models of turbulence and experimental measurements with using hot-wire probe. Normalization was performed dividing the mean value of stream-wise component  $u$  to inlet velocity  $U$ .

The profiles, which were obtained with using different models of turbulence are similar (see Figure 6). The lowest value of normalized stream-wise component of velocity behind the airfoil is near 85 % of  $U$ . This value is valid for SST, BSL RSM and SSG RSM models. Figure 6 shows that the width of the wake region is

similar for models of turbulence, which were used. As for measurement, the lowest value of normalized stream-wise component of velocity behind the airfoil is near 88 % of  $U$ , and the wake region is wider compared with simulations (see Figure 6).

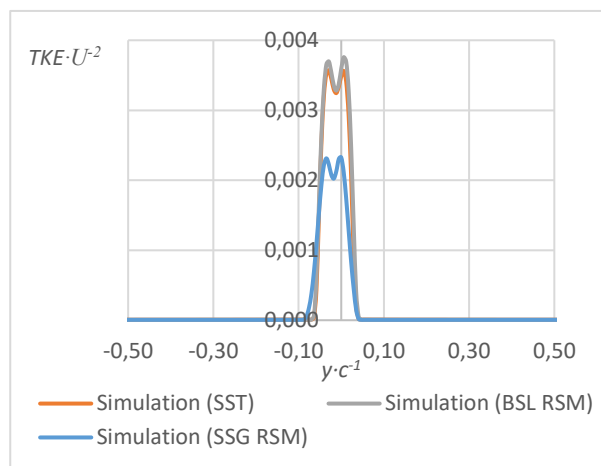


**Fig. 7.** Normalized profiles of Turbulent Kinetic Energy

Figure 7 shows normalized profiles of Turbulent Kinetic Energy ( $TKE$ ) obtained by simulations using SST, BSL RSM and SSG RSM models of turbulence. The values of the  $TKE$  were directly received from simulation. Normalization was performed dividing the values of  $TKE$  to square of the inlet velocity  $U$ . The profile obtained by SST and BSL RSM are almost similar, but the peaks for BSL RSM is 1-2 % higher than for SST model. Also, the distribution of the  $TKE$  for SST is symmetry, it means that this model of turbulence doesn't describe the asymmetry of airfoil. As for BSL RSM, the peaks have small difference near some precents. The peak behind the pressure side ( $y \cdot c^{-1} < 0$ ) is lower than behind suction side ( $y \cdot c^{-1} > 0$ ). As for SSG RSM, the values of  $TKE$  is lower than for values obtained other two models. For SSG RSM the peaks are near 22 % of  $U^2$ , it is by near 30 % lower than the peaks for other models of turbulence. Also, we can say that both peaks for SSG RSM are almost similar. This means that the  $TKE$  distribution obtained by simulation does not or does not sufficiently describe the asymmetry of the airfoil.

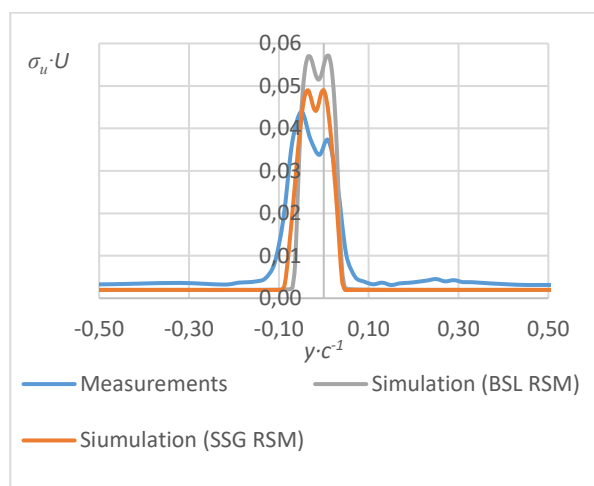


**Fig. 8.** Normalized profiles of standard deviation of stream-wise component of velocity.

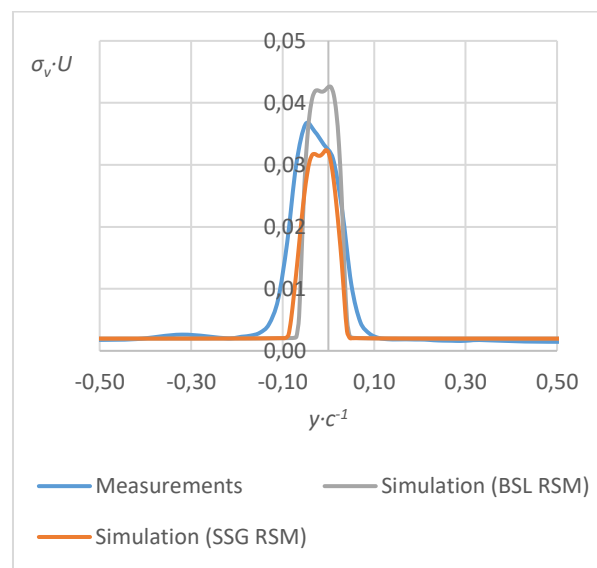


**Fig. 9.** Normalized profiles of standard deviation of span-wise component of velocity.

Figure 8 and Figure 9 show the normalized profiles of the standard deviation of stream-wise and span-wise components of velocity respectively. Normalization was performed dividing the values of standard deviation to inlet velocity  $U$ . The standard deviation were obtained from the experimental and simulated data using BSL RSM, SSG RSM models of turbulence.

Analyzing the Figure 8, it is possible to observe two similar peaks with value: around 5.7 % of  $U$  for simulations using BSL RSM model and around 4.9 % for SSG RSM model. Similarly of peaks means that standard deviation of stream-wise component of velocity doesn't show the asymmetry of the airfoil. As for experimental data, it is possible to observe big relatively difference between peaks. Two peaks have values: 4.3 % of  $U$  behind pressure side and 3.8 % of  $U$  behind suction side. A relatively large peak difference means that the measurements sufficiently describe the asymmetry of the studied profile compared to the simulation. Also, it is possible to see that data obtained by simulation using SSG is more close to measured data than data obtained by simulations using BSL RSM. According to Figure 8, the wake region obtained by measurements is wider compared to the simulations. Analyzing the standard deviation of the span-wise component of velocity shows the difference between measurements and simulation. The values of the peaks for simulations using BSL RSM model are around 4.2 % of  $U$  behind pressure side and 4.3 % of  $U$  behind suction side. As for simulations using SSG RSM model the peaks are around 3.1 % and 3.2 % of  $U$ . The difference of peaks means that the asymmetry of the airfoil during the simulation is possible to observe with helping the profile of standard deviation of span-wise component of velocity. Experimental data have only one peak with value near 3.6 % of  $U$  behind pressure side ( $y/c < 0.1$ ), it means that the measured data describe sufficiently asymmetry of searched airfoil. Also, according to Figure 9 the wake region obtained by measurement is more wider than during the simulations.

## 4 Conclusions

The simulations of asymmetrical NREL's S807 airfoil were performed using ANSYS CFX commercial software with 40 m/s inlet velocity and 0 degree of the accident angle. The numerical investigations were performed using three models of turbulence: SST, BSL RSM and SSG RSM. Simulated data were compared with data obtained by experimental measurements. All data were obtained at cross-section, which is at 100 mm from trailing edge of the airfoil.

The simulated profiles of stream-wise component of the velocity are similar for three models of turbulence. But simulated profiles have relatively big difference with measured profiles. For example, measured profile of the stream-wise component has a lower deficit behind the trailing edge compare with the simulation. Also, the measured profile shows that the wake region is wider compared with the simulations.

The profiles of Turbulent Kinetic Energy were obtained by simulations for three models of turbulence. Each profile has two peaks and they are more higher for BSL RSM model compared to SST, and SSG models. Also, the difference between peaks is absent (SST and SSG RSM) or very small (BSL RSM). It means that these models does not or does not sufficiently describe the asymmetry of the airfoil.

The profiles of the standard deviation of stream-wise and span-wise components of velocity were obtained by measurements and simulations using BSL RSM and SSG RSM models of turbulence. In case of simulation the standard deviation for stream-wise component has two similar peaks and for span-wise the peaks are different. It means that the asymmetry of the airfoil is possible to notice with helping of the profile for standard deviation for span-wise components. As for measured data, the peaks have good visible differences for stream-wise and span-wise components. It means that the measurements show better asymmetry of the airfoil than simulations. Also, the wake region during the measurements is wider compared to simulations.

This work was financial supported by "IDEG Programme", as part of the project Improving the Quality of Internal Grant Schemes at the University of West Bohemia in Pilsen, project reg. No. CZ.02.2.69/0.0/0.0/19\_073/0016931

## References

1. D. C. Eleni, T. I. Athanasios, M. P. Dionissios, Evaluation of the turbulence models for the simulation of the flow over a National Advisory Committee for Aeronautics (NACA) 0012 airfoil, *JMER* **4**, 100-111,(2012)
2. K. K. Koay, W. C. Tan, Computational fluid dynamics study for aerofoil, *Proceedings Of Second National Conference In Mechanical Engineering For Research And Postgraduate Studies*, 2010
3. Y. Seetha Rama Rao et all, *CFD simulation of NACA airfoilsat various angles of attack*, *IOP Conference Series: Materials Science and Engineering* **1**, (2021)
4. F. Menter, J. Ferreira, T. Each, B. Konno, The SST Turbulence Model with Improved Wall Treatment for Heat Transfer Predictions in Gas Turbines, *Proceedings of the International Gas Turbine Congress 2003 Tokyo* (2003)
5. F. Menter, Two-Equation Eddy-Viscosity Turbulence Models for Engineering Applications, *AIAA Journal* **32** (1994)
6. J. Musil, J. Přihoda, J. Fürst, Simulation of supersonic flow trough the tip-section turbine blade cascade with a flat profile, *In Proceedings Topical Problems of Fluid Mechanics 2019*, Prague (2019)
7. *ANSYS CFX-Solver Theory Guide;Release 12.1*; ANSYS Inc.:Canonsburg, PA, USA, 2009.